Performance comparison of two PCM candidates for new concept of compact thermal storage in solar DHW systems

Gilles Fraisse, Maxime Thonon, Laurent Zalewski, Antoine Leconte, Eric Francois, Mickael Pailha, David Cloet, Robert Moracchioli, Luc Traonvouez, Erwin Franquet

PERFORMANCE COMPARISON OF TWO PCM CANDIDATES FOR NEW CONCEPT OF COMPACT THERMAL STORAGE IN SDHW SYSTEMS

Gilles Fraisse*[1], Maxime Thonon[1], Mickael Pailha[1], David Cloet[1], Laurent Zalewski[2], Antoine Leconte[3], Eric François[3], Robert Moracchioli[4], Luc Traonvouez[5]

[1]*Laboratoire Procédés Energie Bâtiment (LOCIE), UMR 5271 (CNRS, Univ. Savoie Mont-Blanc, Chambéry, France*
[2]*Laboratoire de Génie Civil et géo-Environnement (LGCgE), ULR 4515, Univ. Artois, F-62400 Béthune, France*
[3]*Laboratoire d'Innovation pour les Technologies des Energies nouvelles et les Nanomatériaux (LITEN), CEA Tech, Chambéry, France*
[4]*DATE, Développement et Application des Techniques de l'Energie, 38770 La Motte d'Aveillans, France*
[5]*INSULA, 44220 Coueron, France*

**Corresponding author: gilles.fraisse@univ-smb.fr*

Abstract:

The latent heat of phase change allows to increase the energy density compared to sensible storage. In the building sector, it is possible to replace hot water tanks that are bulky due to their cylindrical shape, by smaller storage volume and parallelepiped geometry. The idea of the new concept is thus to propose a hybrid and modular storage component with a cavity containing the phase change material (PCM) delimited by two flat heat exchangers connected by slotted fins. The first step was to precisely characterize the behavior of the two selected PCMs during melting and solidification, without and with supercooling (respectively RT58 and PEG6000). The next step concerns the modeling of the storage cavity and then the optimization of the new full-size concept for solar domestic hot water systems. A prototype was experimentally tested for the two PCMs under real operating conditions with a reduced sequence of six days allowing the annual performance to be calculated.

The experimental results confirm the known limit of PCM concerning its low thermal conductivity, which can penalize the power extracted from the storage during continuous withdrawals. The spacing of the fins thus plays a major role in heat transfer. The evaluation of the annual performances carried out on the prototype shows that the solar fraction is quite satisfactory, between 40 and 90% depending on the climate in France. The distribution of average temperatures observed within the PCM is directly correlated with the melting ranges. The RT58 is thus penalized compared to the PEG6000 because the start of the melting takes place at a much lower level (30°C against 52°C), which can lead to more frequent use of back-up. Regarding heat storage, the much lower density of the RT58 explains the difference in energy stored in the prototype (+34% for the PEG6000 between 20 and 80°C) knowing that the latent heat and the specific heat are of the same order of magnitude in both cases. Finally, the higher thermal conductivity of PEG6000 favors the heat rate exchanged during the storage charging and discharging phases.

Keywords: PCM – Latent heat storage – Experimental characterization – Inverse method – Solar domestic hot water system

Nomenclature

Variables

C_{eff}	$Effective\ heat\ capacity, J.kg^{-1}.K^{-1}$
Cp	$Sensible\ heat\ capacity, J.kg^{-1}.K^{-1}$
E	$Energy, J$
f	$Liquide\ fraction$
h	$Enthalpy, J.kg^{-1}$
L	$Latent\ heat, J.kg^{-1}$
R	$Thermal\ resistance, m^2.K.W^{-1}$
T	$Temperature, K$
t	$Time, s$

Greek letters

β	$Heating/Cooling\ rate, K.min^{-1}$
ΔT	$Temperature\ variation$,°C
ϕ	$Heat\ flux, W$
λ	$Thermal\ conductivity, W.m^{-1}.K^{-1}$
ρ	$Density, kg.m^{-3}$

Acronyms

DHW	$Domestic\ hot\ water$
PCM	$Phase\ change\ material$
SF	$Solar\ fraction$

1. Introduction

It is now established that limiting climate change and its consequences requires reducing greenhouse gas emissions. The objective of carbon neutrality in 2050 will make it possible to limit the rise in temperature, provided that a major effort is made to reduce energy consumption. With the war in Ukraine, rising energy costs and supply difficulties led to the urgent development of energy conservation plans covering the energy consumption of buildings and transports in many European countries. As the building sector is the main consumer of energy, it is important to launch a large-scale renovation of buildings, to improve the efficiency of energy systems and to use solar energy which is an intermittent source. Solutions must also be identified regarding adaptation to climate change, for example by ensuring thermal comfort during heat waves. In this context, thermal storage is a central element that makes it possible to limit temperature peaks in buildings thanks to the inertia of the walls, or to take benefit from solar energy. As a result, it can also be used to shift the load demand from peak hours to off-peak hours of the day. It is no secret that latent storage offers a higher energy storage capacity than sensible energy storage for the same volume.

The subject addressed in this article relates more specifically to thermal storage with phase change materials (PCM) for the production of solar hot water. The objective is to replace hot water tanks, which are bulky due to their cylindrical geometry, with more compact latent storage and a parallelepipedal geometry. Reducing clutter is essential in existing buildings to add new solar storage during renovations, and in new buildings because the real estate cost leads to the rationalization of surfaces. The current industrial storage products for solar hot water systems with PCMs only are very limited. One of the reasons is the complexity due to the presence of two heat exchangers coupled to the PCM storage. The load exchanger is connected to the thermal solar collectors. Charging takes place when the temperature difference between the solar collector and the storage becomes greater than a previously defined threshold. The discharge exchanger is connected to the domestic hot water (DHW) system and operates at each tapping. We have only identified the company SUNAMP which offers storage batteries allowing this mode of operation in simultaneous charging and discharging, with storage capacities between 3.5kWh and 12kWh.

Regarding scientific studies, we rule out hybrid water-PCM solutions that are developed to increase storage capacity or promote stratification [1] [2] [3]. The framework of our study concerns storage solutions with PCM only and two heat exchangers allowing simultaneous charge-discharge. Two main categories can be defined. These are on the one hand integral collector storage with PCM positioned outside, particularly on the roof [4] [5] [6], and on the other hand storage units with cylindrical [7] or parallelepipedal [8] geometry, positioned inside the building.

It appears from this bibliographic work that storage cavities with PCM solar thermal systems are very little studied, which may also explain the lack of industrial offers. It is necessary to propose innovative concepts operating in simultaneous charging and discharging, with possible direct transfer between the two heat exchangers (solar loop and DHW). The development of new hybrid storage and transfer concepts also comes up against often imprecise PCM behavior laws (with and without supercooling) [9]. Under these conditions, the energy performance estimated numerically may lack reliability. Thus, this is detrimental to the development of solar storage with PCM

because the demonstration of its interest is difficult compared to the solar hot water tank which works very well in terms of energy performance, even if its size is larger.

This article thus presents the development of a new concept of storage with PCM for solar thermal systems for the production of DHW. The work is based both on PCM characterization methods based on flux measurements [10], [11], [12], [9] [13] and annual system performance evaluation methods based on reduced test sequences [14].

The selection of PCM candidates for heat storage must consider the melting temperature (close to the setpoint, i.e. approximately 55°C), as well as the ability to store (latent heat, specific heat and density) and transfer heat (thermal conductivity). Other aspects must also be considered such as the degree of supercooling and the possible risks (sanitary, segregation, corrosion, etc.). From these selection criteria, we finally selected a polymer (PEG6000) and a paraffin (RT58). In the first part, the article presents the analysis of the thermodynamic behavior of these two PCMs and their ability to store heat for the targeted DHW application. The characterization of the PCM is carried out on a fluxmeter bench by energy balance and inverse methods. This approach gives access to all the thermo-physical characteristics and the PCM behavior laws (enthalpy, liquid fraction and equivalent specific heat) as a function of temperature. The comparison of the two PCMs for heat storage is proposed in a second part in charge and discharge for a cavity comprising fins in order to increase heat transfer. The analysis of the differences observed on the energy stored and the powers exchanged in charging and discharging is based on the characteristics of the PCMs previously identified. The third and final part begins with the presentation of the hybrid PCM storage and exchange component, designed to allow simultaneous charging (solar) and discharging (DHW), as well as direct transfer between the two heat exchangers (solar and DHW) thanks to the fins. The evaluation of the annual performance of the new storage concept on a semi-virtual test bench from a reduced sequence of six days is finally proposed for the two PCMs. The final choice of the best PCM for the considered application is finally proposed, as well as ways to improve the performance of the prototype.

2. Ability of the two PCM candidates to store heat

2.1. Preliminary question: is PCM storage relevant?

A preliminary question before selecting a PCM storage is to clearly identify its interest compared to conventional storage. In the case of solar DHW systems, water constitutes a solution that is difficult to compete for financial reasons (cost of water vs. PCM) and ability to store heat (high specific heat for water). The relevance of the PCM is mainly motivated by the compactness which is an interesting criterion with regard to the cost of real estate (€/m²) both in new construction and renovation. During an energy renovation, adding solar storage can also be difficult for reasons of available space. Compactness is in this case an important criterion for the very feasibility of the project. A big advantage of PCM is its ability to store heat for small temperature differences. In the case of solar storage, temperature differences are limited because the temperature range in the storage will tend to be higher in summer (typically 40-80°C) than in winter (20-50°C). Other applications require a limited temperature operating range, such as the batteries of electric vehicles. In this case, the PCMs make it possible to passively manage the temperature of the components thanks to an adapted melting temperature.

Other characteristics of PCMs can be useful. For example, the rise in temperature before the start of melting makes it possible to reduce the use of back-up in a solar DHW system because the desired setpoint temperature can be obtained more quickly (sensible heat energy is lower than latent heat). It is also possible to take advantage of supercooling to reduce heat losses over long periods [15] [16]. Concerning the health issue, legionella risk is ruled out because the water drawn is not stored and water storage may not be accepted in certain countries if it presents significant health risks.

A number of disadvantages of PCMs should be carefully considered. Their low thermal conductivity is a point of vigilance if the heat rates are high. In the case of solar storage, the heat extracted from the collectors is transmitted gradually during the day to the storage. The low conductivity of PCM is not penalizing in this case. On the other hand, the production of domestic hot water requires high discharge powers (20 to 25kW for an individual house boiler in instantaneous heating). It is important in this case to promote heat transfer by adjusting the equivalent thermal conductivity. There are many possibilities for intensifying transfers [17] [18] [19] [20]: fin spacing, nanoparticles, metal foam, etc. The expansion of PCM during melting, and vice versa during solidification, also does not play in favor of the power extracted due to the presence of additional contact resistances during discharge. A final point to consider for a DHW storage system is the impact of the number of charge-discharge cycles. The choice of the PCM must of course integrate the stability of the thermo-physical characteristics over time.

The two main factors limiting the use of PCMs are certainly the cost and their low thermal conductivity. Nevertheless, the cost of the PCM is not necessarily preponderant with regard to the cost of the complete installation. This is what we observed in the case of a solar hot water production system with PCM [21]. The cost of PCM is about 25% of the cost of storage. If we consider the cost of real estate and the reduction in occupied space, the financial gap is necessarily reduced between the hot water tank and the PCM storage.

We have found that the MCP behavior laws usually used are not particularly reliable [9] for both melting and solidification, and that characteristics such as supercooling are generally poorly modeled, particularly during partial melting-solidification cycles. It is important to accurately characterize the behavior of PCMs to show their interest compared to a hot water tank. The comparison of the two PCMs proposed in this article is thus based on finer characterization methods than those usually considered in the literature [9] [13] [22]. This is an important step in trying to "democratize" PCMs in the building sector, particularly with the current trend of moving towards bio-based PCMs with behaviors that can be more complex than paraffins for example.

2.2. Selection of the two PCM candidates

In this study, which concerns a solar DHW system, the specifications relating to the choice of PCMs are quite simple. Latent heat, sensible heat and density should be maximized, while minimizing cost. Given the intended application, the melting temperature must be close to 55°C and the numerous charge-discharge cycles must not alter the thermo-physical properties with, for example, the appearance of segregation phenomena. We have thus selected two PCMs whose characteristics provided by the manufacturers are presented in Table 1.

PCM	Latent heat ($kJ.kg^{-1}$)	Phase change temperature (°C)	Specific heat ($kJ.kg^{-1}.K^{-1}$)	Density ($kg.m^{-3}$)	Thermal conductivity ($W.m^{-1}.K^{-1}$)
RT58 (Paraffin)	*160*	*53-59*	*2*	*0.88*	*0.2*
PEG6000 (Polymer)	*192*	*55-62*	*2.3*	*1.2*	*0.3*

Table 1: Data provided by the manufacturers for the two PCMs studied

This information is not sufficient to assess the energy efficiency of the two PCMs in the intended application. A characterization work was thus carried out in order, on the one hand, to verify the data provided by the manufacturers, and on the other hand to define the precise behavior laws of the two PCMs selected as a function of the temperature. A simple bibliographical analysis shows that the behavior laws available in the literature are not compatible with these two PCMs:

- A mixture of two components or crystalline structures leading to more complex characteristic curves as a function of temperature for the enthalpy *h(T)*, the liquid fraction *f(T)* and the equivalent specific heat *Ceff(T)*. We have clearly observed the limits of the models available in the literature in the case of RT-58 [9]. The new proposed laws have been validated experimentally in the case of temperature ramps and steps (both heating and cooling modes).
- Supercooling is rarely modeled accurately. We have thus defined a heat diffusion law during the recalescence phase, as well as the complete solidification curves which depend on the cooling rate. Regarding the partial charge and discharge cycles, a reference cooling curve and the melting curve make it possible to determine the intermediate states thanks to the “curve scale” method [23] [24]. Tests on a fluxmeter bench in melting and complete or partial solidification, for different heating and cooling ramps were carried out with the PEG6000. The dynamic model and the experimental results obtained were presented in [13].

The following part presents the comparison of the behavior laws of the two selected PCMs. These results will be useful to analyze later on the one hand their ability to store heat in a cavity, and on the other hand their level of performance in a real storage system for the production of solar hot water.

2.3. Characterization of the two PCMs

2.3.1. Characterization by inverse method on fluxmeter bench

The first step consists in characterizing the behavior of PCM during melting and solidification (RT58 without supercooling and PEG6000 with supercooling). Some parameters are identified by energy balance (specific heat and latent heat) and others by the inverse method (thermal conductivity). This last method is also used to determine the enthalpy *h*, the liquid fraction *f* and the equivalent specific heat *Ceff* as a function of temperature. The behavior laws presented in [9] and [13] for the two PCMs do not include certain invalid assumptions that are often considered in the literature: linearity of *f(T)*, discontinuity or symmetry of *Ceff(T)* and single component. Analytical equations related to *h(T)*, *f(T)* and *Ceff(T)* characteristics have been proposed for complete and partial melting/solidification cycles (without and with supercooling). In the presence of supercooling, the temperature of

the onset of crystallization and the complete solidification curves are identified as a function of the cooling rate β. This same parameter is used to determine the duration and the variation of the heat release during the recalescence phase. The partial cycles are defined from a reference cooling curve and that of complete melting. The intermediate states between these two limits are obtained with the "curve scale" method [23] [24].

A fluxmeter experimental bench was built to characterize the selected PCMs. It makes it possible to apply thermal boundary conditions like ramps, using baths at constant temperature, on a parallelepipedal briquette of 21*14*1.8 cm^3 in acrylic (PolyMethyl MethAcrylate) containing the PCM. A volume of 0.3 liters of PCM (200g to 300g) is characterized, a much larger quantity than for usual DSC measurements (a few mg). The instrumentation of the test bench includes tangential gradient flow sensors which are located on each side of the sample, between the outer wall of the briquette and the flat exchanger. The flow sensors, manufactured by the CAPTEC company, have the same area as the faces of the briquette, a thickness of 0.2mm and a sensitivity of 117µV.W.m². Once calibrated, the uncertainty of the measurement is around 3%. A type T thermocouple is also located into the PCM halfway up the briquette. This direct measurement of the PCM temperature is very useful because it allows on the one hand to better observe certain phenomena such as the recalescence phase, and on the other hand to validate the models more precisely by considering both the flow measurements at surface boundaries and temperature within the PCM.

2.3.2. Example of complete melting and solidification cycle

An example of the response of the two PCMs is shown in Figure 1 during melting and solidification ramps lasting 4 hours. The surface temperature is set and the heat flow are measured, as well as the temperature within the PCM. The two PCMs show very different behaviors regarding their melting range (30-62°C for RT58 and 52-64°C for PEG6000) and supercooling which is particularly present in the case of PEG6000 (a dozen degrees). The recalescence phase is observed over a period of approximately 1500 seconds with the increase in the temperature of the PEG6000 during cooling. Figure 1 shows that the stored energy and the maximum heat flows exchanged are higher in the case of the PEG6000. These results are consistent with the data proposed by the two manufacturers, if we compare the values related to storage (specific heat, latent heat and density) and heat transfer (thermal conductivity). We will see later with a more precise characterization that it is mainly the difference in density that explains the differences in the stored energy.

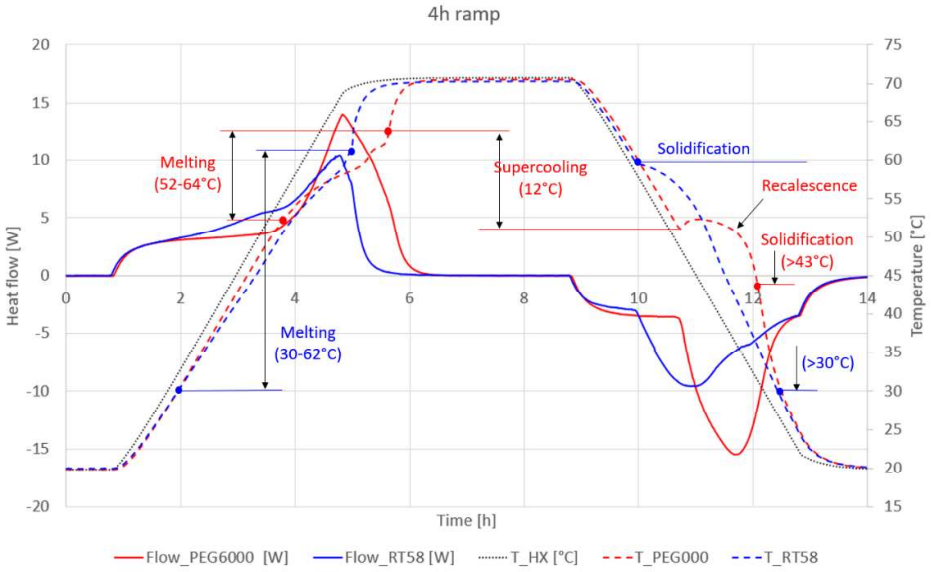

Figure 1: Evolution of heat flows and temperatures (set on the briquette boundary surface and measured in the PCM) during a complete melting and solidification cycle (duration 4 hours; PEG6000 and RT58)

2.3.3. Main parameters identified with fluxmeter bench

The characteristics obtained (table 2) show that the main difference concerning energy storage is the density (factor 1.4 in favor of PEG6000) because the specific and latent heats are of the same order of magnitude (the values for the latent heat were very different with the data provided by the manufacturers). The fluxes exchanged are higher in the case of PEG6000 (figure 1) because the thermal conductivity is greater (factor 1.7 in the solid state). In

melting, the phase change range is much smaller for PEG6000 than for RT58. This means that the rise in temperature towards the storage set-point temperature (approximately 55°C) is faster for the PEG6000.

Characteristics		Units	RT58	PEG6000
Density	ρ	kg.m^{-3}	880	1200
Thermal conductivity	λ_S λ_L	*W.m^{-1}.K^{-1}* *W.m^{-1}.K^{-1}*	*0.206* *0.237*	*0.35* *0.41*
Specific heat	Cp_S Cp_L	*J.kg^{-1}.K^{-1}* *J.kg^{-1}.K^{-1}*	*2112* *2100*	*1914* *2100*
Latent heat	*L*	*kJ.kg^{-1}*	*172.4*	*172.5*
Melting range		*°C*	*30>62*	*52>64*
Solidification range		*°C*	*60>30 °C*	*>43°C*
Supercooling	ΔT	*°C*	*Faible*	*= 11.5 à 12.5°C*
Recalescence duration	Δt	*s*		*1000-3000*

Table 2: Main characteristics obtained by energy balances and inverse methods for the two PCMs studied

Figure 2 illustrates the results of table 2 concerning the energy density stored during melting, with a simplified (linear) representation of each state (solid, solid-liquid mixture and liquid). Compared to water, PEG6000 stores for the same volume 2.22 times more energy during a charge between 40 and 70°C (factor 1.56 between 20 and 70°C). In the case of the RT58, the factors are 1.59 and 1.17 respectively. Between the PEG6000 and the RT58, the factors are respectively 1.40 and 1.34 for the temperature ranges 40-70°C and 20-70°C. PEG6000 has a higher mass density than RT58 (factor 1.36); which largely explains the differences in energy density stored between these two PCMs. It is easy to observe that the interest of the PCM compared to water depends on the temperature difference during the charge, and that the PEG6000 is clearly more efficient. If we consider a summer period, the temperature will be higher (typically 40-70°C) and the PEG6000 will be able to store much more energy than water in this case (factor 2.22) . In winter, the available solar energy is low and the temperature in the solar storage is lower (range around 20-40°C). For the same quantity of solar energy transmitted to storage, the temperature rise will be greater for PEG6000 (solid state up to 52°C), compared to water (high specific heat) and RT58 (melting starting at 30°C).

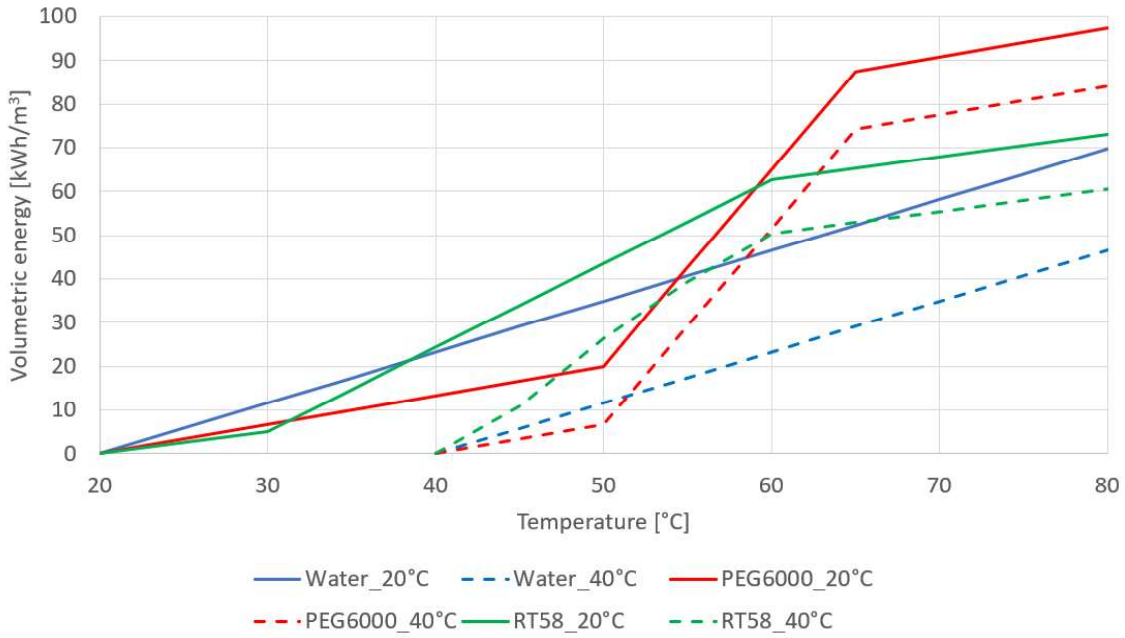

Figure 2: Simplified representation of the volumetric energies stored during charge, according to the characteristics identified with the fluxmeter bench (table 2)

2.3.4. Comparison of behavior laws

The parameters identified in Table 2 are not sufficient to correctly model storage with PCM. The dynamics of the phase change (fusion and solidification) must be specified as a function of the temperature. The behavior laws must also show in the case of RT58 a solid-solid transition followed by a solid-liquid transition [25], as well as

supercooling for PEG6000. This is possible by identifying either the enthalpy *h(T)* shown in Figure 3, or the liquid fraction *f(T)* or the equivalent specific heat *Ceff(T)*. Only one of these three quantities is sufficient to obtain the other two by applying the following relationship:

$$Ceff(T) = Cp + L * \frac{df(T)}{dT} = \frac{d\mathbb{P}(T)}{dT} \quad (1)$$

The *h(T)* curves identified with the fluxmeter bench for the two PCMs are quite different, as shown in Figure 3 in the case of an 18-hour ramp [22]. The behavior is similar for RT58 between melting and solidification (very slight supercooling). On the other hand, a significant difference is observed for PEG6000 due to supercooling (approximately 12°C) that depends on the cooling rate. The hysteresis in the case of PEG6000 leads to a more complex behavior during partial melting and solidification cycles. The shape of the *h(T)* curve leads to the presence of two peaks for *Ceff(T)* which are very marked for PEG6000 (peaks at 57 and 62°C) and less marked for RT58 (peaks at 45 and 60°C). These results can be observed in [9].

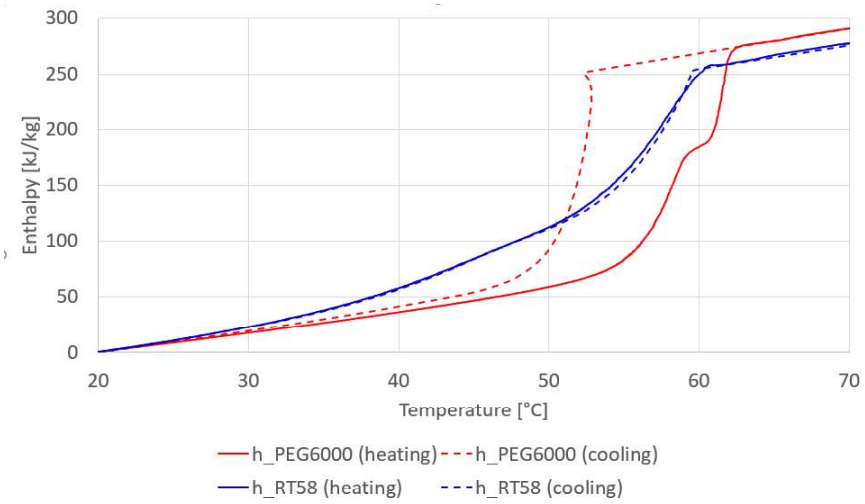

Figure 3: Comparison of behavior laws (enthalpy) during melting and solidification for the two PCMs (ramp duration : 18h)

An important common point between these two PCMs is the similar order of magnitude of the latent heat L [J/kg] (Table 2). Manufacturer data is underestimated for RT58 and overestimated for PEG6000. If we compare the enthalpy of the two PCMs between 20 and 70°C, the PEG6000 (290.7kJ/kg) stores during melting 1.05 times more energy than the RT58 (277.6kJ/kg), and 1.16 between 40 and 70°C (254.6/219.8kJ/kg). Between 20 and 70°C, the mass energy stored is therefore of the same order of magnitude. The slightly higher factor between 40 and 70°C is explained by the melting range which starts earlier in the case of the RT58; meaning reduced latent heat exploited.

3. Study of the charge and discharge of a storage cavity with fins

After comparison of the two PCM characteristics identified on a fluxmeter bench, and of the ability to store energy initially thanks to the evolution of the volumetric energy (figure 2) during melting calculated from table 2, then from the enthalpy *h* [J/kg] as a function of temperature (figure 3), a cavity filled with PCM is studied considering temperature steps for charge and discharge (20>70 >20°C). The results obtained are analyzed with regard to the characterizations carried out beforehand.

3.1. Description of the device

The cavity containing the PCM is parallelepipedal with dimensions of 25cm*25cm*4cm (Figure 4). A total of 34 aluminum fins 0.5mm thick connect the two sides of the cavity. The spacing of the fins is thus 7.5 mm and their length equal to the thickness of the cavity, i.e. 4 cm. The fins allow above all to increase the effective thermal conductivity of the PCM. A set of seven thermocouples gives the evolution of the average temperature of the PCM contained in the cavity (RT58, and then the PEG6000).

Figure 4: The studied cavity containing the PCM (PEG6000 and RT58)

The characterization of the studied cavity is carried out by heat flux measurement, with a test bench similar to that used for the characterization of PCMs. Two heat exchangers set temperature (ramp or step) on the two aluminum faces of the cavity. Heat flow sensors, located between the outer wall of the cavity and the heat exchanger, are used to measure the heat fluxes exchanged between the storage cavity and the exchangers. Several thermocouples are placed in each cavity to monitor the evolution of the temperature in the different cells and at different heights. For each cavity, a thermocouple is located at the lower quarter of the cavity, five thermocouples at mid-height, and one thermocouple at the upper quarter. Flow and temperature measurements are measured every 10 seconds.

3.2. Comparison of energies exchanged during charge and discharge

The experimental results show a stored energy [kJ] in the cavity volume 1.38 times greater for PEG6000 between 20 and 70°C mainly due to the density ratio (1.36). This result is consistent with the evaluations made from the simplified linear representation in figure 2 (factor 1.34 between 20 and 70°C).

As expected, the temperature rise observed in figure 5 is faster for PEG6000 than RT58 due to the latter's wider melting range starting at 30°C (figure 1). The fluxes exchanged are higher for the PEG6000 than the RT58 given the differences in thermal conductivity (factor 1.7 between the PEG6000 and the RT58) and the quantities of energy exchanged. Higher thermal conductivity intensifies exchanges and reduces phase change times. The average fluxes exchanged in fusion Φ_{FUS} and solidification Φ_{SOL} can be evaluated from the energies stored and the durations of fusion-solidification:

$$\Phi_{FUS\_PEG} = 1.65 * \Phi_{FUS\_RT} \quad \text{et} \quad \Phi_{SOL\_PEG} = 1.84 * \Phi_{SOL\_RT}$$

A first flux peak for the two PCMs is observed during charge and discharge, linked to the rapid destocking effects of the fins and a thin layer of PCM. Given the higher conductivity of PEG6000, the duration of this first flux peak is a little longer. The second peak lasts longer for the two PCMs because it is related to fusion, a slower phenomenon. The maximum value of the second flux peak is larger in the case of PEG6000 due to the narrower melting range. During discharge, the PEG benefits from the heat flux released by the PCM during the recalescence phase. An average value of this flux linked to the recalescence phase can be evaluated. Indeed, the enthalpy curve during solidification was identified by considering three steps: cooling until the beginning of nucleation at a temperature below that of the liquidus, phase of recalescence and continuation of solidification. The proportion of latent heat dissipated during the recalescence is easily evaluated at the end of the first step. It is about 15% of the latent heat in the case of PEG6000, i.e. about 27500 J/kg dissipated over a period of about 1500 seconds. This corresponds to 52W dissipated on average (15% * 172500J/kg * 0.25^2 * 0.04 * 1200kg/m^3 / 1500s) which represents 20% of the maximum flux (250W). The variation of heat flow shows that phase changes are generally slower in melting than in solidification.

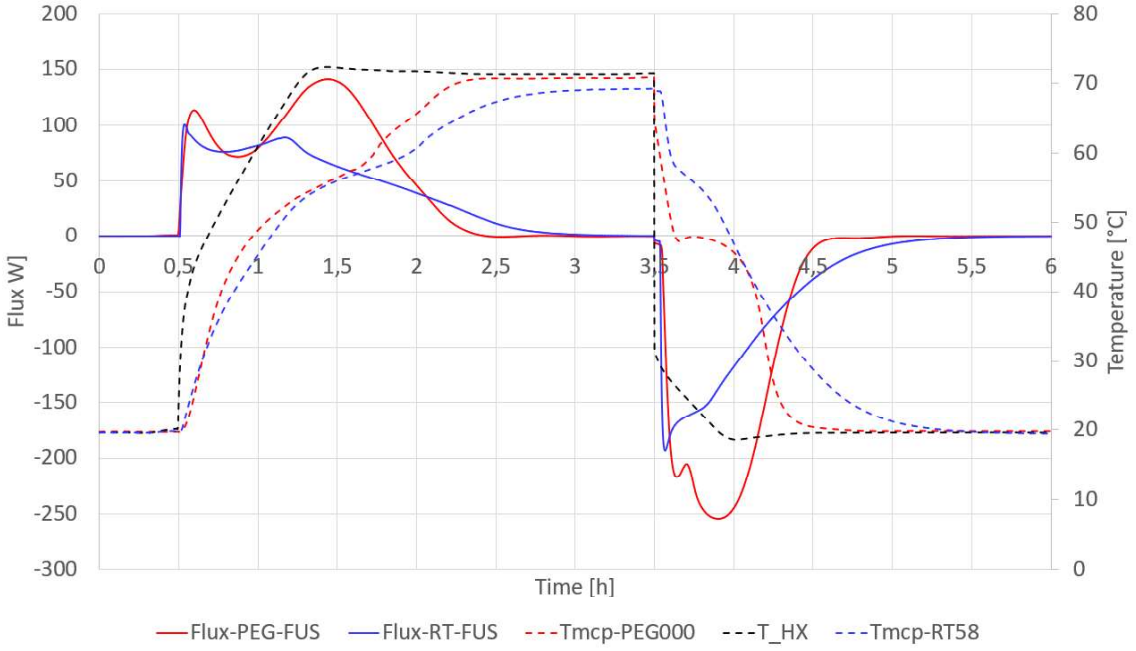

Figure 5: Evolution of heat flux and temperatures during charge-discharge with temperature steps (20-70°C and 70-20°C) for PEG6000 and RT58

4. Evaluation of the annual performance of a solar SDW system

4.1. Presentation of the prototype

The new concept was developed for a solar domestic hot water system in a single-family house. It integrates the PCM storage and two heat exchangers allowing solar charging and hot water drawing. Direct exchange is possible during simultaneous charging and discharging (figure 6). The basic component is the cavity providing storage (PCM) and heat transfer (fins). The coupling of this cavity with two flat heat exchangers located on each face constitutes a module. These heat exchangers ensure the charge (solar loop) and the discharge (DHW) of the PCM storage. They meet specifications related to the powers to be transferred, cost, mechanical strength, health risks, corrosion and weight. In addition to allowing direct transfers between the two heat exchangers during simultaneous charge-discharge, the main role of the cavity fins is to increase the effective thermal conductivity of the PCM. Thus, the spacing of the fins is the factor allowing to adjust the effective conductivity, and therefore the discharge power. The storage is modular since the storage capacity can be adapted by combining different modules which share the solar and DHW exchangers.

A 2D model of the new full-size concept for a solar hot water production application made it possible to propose a set of optimal configurations considering energy performance and cost [21]. The compromise solution adopted served as the basis for defining the prototype which was built by coupling four modules. Each of the four modules has a volume of 70*70*5cm^3 and they are placed in a sealed tank. In total, two heat exchangers are used for solar charging, and three for discharging (DHW). The prototype was tested on a semi-virtual test bench in order to compare it with a classic hot water tank modeled with the TRNSYS software. The experimental evaluation of annual performances is possible thanks to the use of a real six-day sequence obtained with the TYPSS algorithm [14]. The six-day sequence makes it possible to reproduce with precision the annual performances of the classic system simulated with TRNSYS. The weather conditions of Nice (southeast of France: Mediterranean climate), Lyon (mid France) and Strasbourg (East of France: Continental climate) were considered.

Figure 6: View of the interior of the prototype with the four cavities, the fins and the 5 plate heat exchangers

The prototype was sized considering half solar storage (i.e. 100 liters of PCM equivalent to 150 liters of water) knowing that the volume of a solar tank is approximately 300 liters of water. The power required during discharge for a complete storage of DHW is around 25kW considering the possible withdrawal rates (700l/h) and the temperature differences considered. The three DHW heat exchangers used in the prototype were sized to provide half of this power, with the assumption that two prototypes would be required for the full installation. The two solar exchangers are identical to the three DHW exchangers. The surface of solar collectors coupled to the prototype is 2.5m² and 100 liters of hot water are drawn off each day (equivalent to half an installation or a dwelling occupied by 2 people). The solar power transmitted by the solar collectors being at most 2.5kW, we can consider that the two solar exchangers are rather oversized.

Each of the five heat exchangers is made up of two 0.5mm stainless steel sheets (1 flat and one stamped with spot welds over the entire surface for pressure resistance, as well as a weld on the periphery for sealing). The channel between these two plates is 1mm. In the cavity, the pitch of the fins is 6mm. The thickness and length of the fins are 0.3mm and 5cm respectively. The volume of each cavity is 24.5 liters (98 liters for the four cavities). A total of 94 liters of PCM are used (83 kg of RT58 and 112 kg of PEG6000) and the aluminum fins weigh a total of 15 kg. The total weight of the five heat exchangers is 20 kg. The total thickness of the prototype (without the 10cm thick insulation) is 22cm. The energy stored per module (prototype = 4 modules) is between 2 and 2.5kWh ($70*70*5cm^3$) for the PEG6000, and between 1.5 and 2kWh for the RT58 depending on the temperature range considered. The prototype can be used in two hydraulic configurations:

- Prototype with a high power back-up (this is the configuration tested experimentally);
- Prototype with a low-power back-up (existing electric hot water tank in the event of solar renovation, for example).

4.2. Evaluation of annual performance on a semi-virtual bench

The objective of the tests is to assess the annual performance of the prototype integrated into a solar DHW system. For this, the prototype is installed on the CEA-INES "semi-virtual" test bench. The prototype's two heat exchangers are connected to hydraulic modules that dynamically reproduce the behavior of a field of solar thermal collectors and DHW draw-offs, as well as instant back-up if the outlet temperature is below the setpoint. The "virtual" environment is thus interacting with the prototype in real time. It experimentally reproduces the behavior of the elements outside the prototype: the temperature of the cold water network, the temperature at the outlet of the solar collectors according to the climatic conditions and the outlet temperature of the solar exchanger of the prototype, the auxiliary power which heats the fluid at the outlet of the prototype up to the set point of 50°C, and finally the mixing valve which makes it possible to provide a DHW temperature of 40°C.

The test bench is equipped with numerous sensors (volumetric flow, temperature, power, pressure), with in particular those required in the standards NF EN 12977-3 and NF EN 12897. All the probes have been calibrated with their complete acquisition chain. The temperature measurements on the test bench and the hydraulic modules are carried out with Pt100. The measurement uncertainties are of the order of 1 to 2/10th of a degree. The acquisition time step is 10 seconds. The experimental installation is shown in Figure 7 in which T represents the temperature measurements on the different hydraulic circuits. The prototype is also equipped with many internal thermocouples to measure the temperature of the material during system operation.

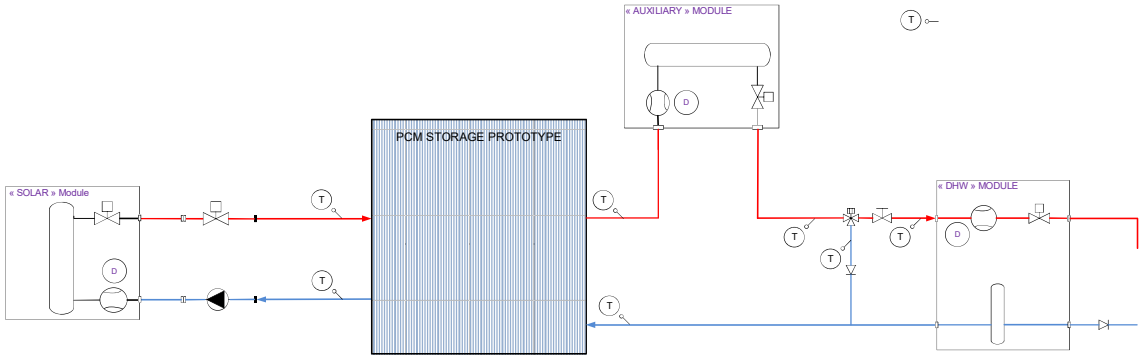

Figure 7: Diagram of the experimental bench

Scenarios considered in the evaluation of the annual performance of the system are based on the TYPSS methodology [14]. It has been developed with the aim of extracting an annual profile of input data (climatic variables and water draws in this case) a typical short sequence allowing the precise reproduction of the behavior of a numerical model and, by extrapolation, its annual performance. The TYPSS algorithm relies on numerous Dynamic Thermal Simulations of a reference case to select the typical days. The prototype model is not adapted to the algorithm because of the very high calculation times due to the phase change and the spatial discretization. The model considered is thus that of a classic solar water heater, simulated with TRNSYS, whose expected behavior is similar to that of the prototype. For practical reasons, the test sequence should be as short as possible. This allows more tests to be performed in a given time and minimizes the interruption of the test sequence for various reasons. Several TYPSS sequences were thus generated, with durations ranging from 4 to 12 days. The 6-day TYPSS sequence offers the best compromise to obtain sufficiently accurate estimates (3% overestimation of the annual solar yield and 4% of the energy saving rate) in a short time. It was generated for the climates of Strasbourg (East of France: Continental climate), Lyon (mid France) and Nice (southeast of France: Mediterranean climate).

4.3. Experimental results

4.3.1. Stored energy and annual solar fraction

Figure 8 presents the energy balances over one year for the solar energy collected (Ecoll), the energy required to meet DHW needs (Edhw) and the energy supplied by the back-up system, as well as the performance criteria (solar collector efficiency Eff and solar fraction SF) for each climate and the three cases considered:

- TYPSS: numerical results by applying the TYPSS sequence to the classic reference solar DHW system
- EXP_RT: experimental results obtained by the prototype filled with RT58 with the same TYPSS sequence
- EXP_PEG: experimental results obtained by the prototype filled with PEG6000 with the same TYPSS sequence

The results show that the prototype (experimental data EXP_RT and EXP_PEG) stores as much solar energy (Ecoll) as with a conventional water tank (TYPSS), but with a smaller volume (100 liters of PCM and 150 liters for water). If we consider the size due to a cylinder that fits into a parallelepipedal volume, the factor is 1.9 ($1.5*4/\pi$). The auxiliary energies truly reflect the performance of the solar installation. They are generally higher for the prototype (PEG6000 and RT58) than for the classic tank. This is the reason why the solar fraction (SF) varies between 43% and 87% depending on the climate for the two PCMs which present similar results, while the classic system gives higher values, between 64% and 91 %. The lowest values correspond to the climate of Strasbourg and the highest to Nice; Lyon being an intermediate configuration.

The slightly lower solar coverage of the prototype is probably linked to the maximum flow rate considered during the experimental tests of the prototype. They are quite high (700l/h) given the sizes of the three DHW heat exchangers for which half storage was considered (i.e. 350l/h). We will see later that it is quite possible to meet the 25kW (for 700l/h) with the prototype by adjusting the spacing of the fins. Of course, storage with water is not penalized by the withdrawal power because the hot water can be drawn directly from the storage. Overall, RT58 and PEG6000 have similar annual performance despite the advantages of PEG6000 that have been put forward (narrower melting range; higher thermal conductivity and latent heat). The reason is due to the fact that they have the same limiting factor: a high maximum flow rate with regard to the sizing of the DHW heat exchangers requiring the use of back-up. Despite this, the solar coverage obtained with the prototype is quite satisfactory (43% to 87%).

It is interesting to note that in Nice, the solar fractions are close between the PEG6000 (87%) and the water (91%), while the RT58 gives a significantly lower result (74%). The reason is linked to the higher temperature levels reached in storage with PEG6000 (generally between 50 and 70°C) which allows the PCM to remain permanently in liquid form. Thus, the thermal conductivity is greater (see table 2) and better heat exchanges take place between the PEG6000 and the fins thanks to the lower superficial resistances. Under these conditions, supercooling plays a positive role in energy performance by allowing PCM to remain liquid longer. Finally, the annual efficiency of the solar collectors *Eff* logically follows the evolution of the energies *Ecoll* transmitted to the storage by the collectors.

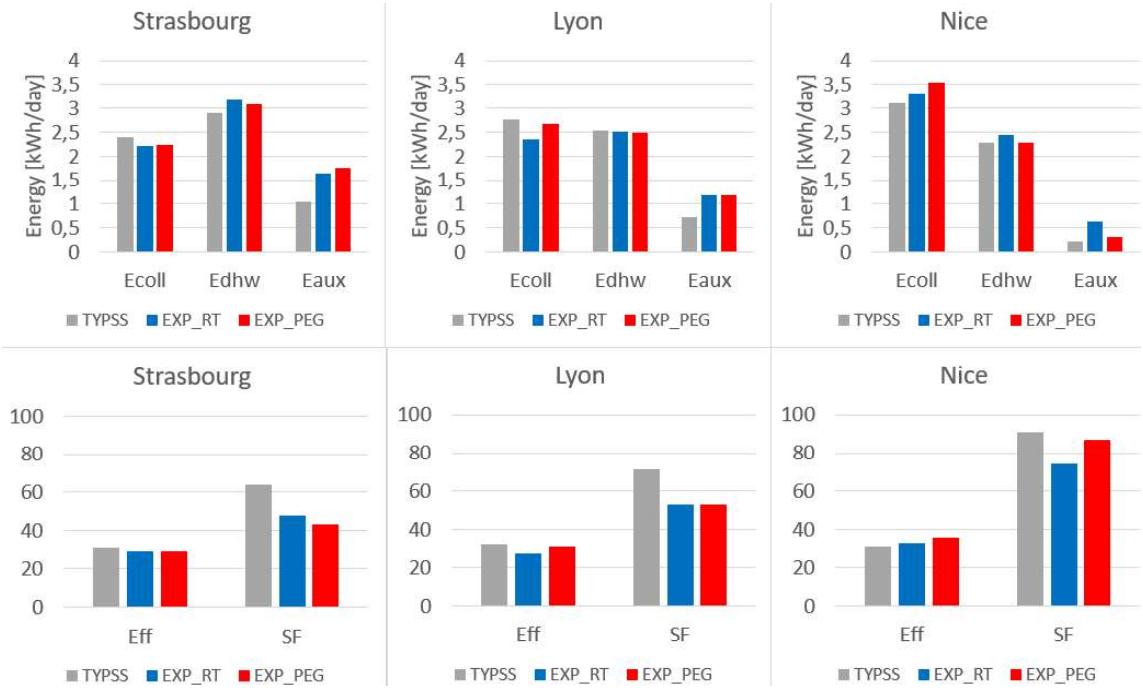

Figure 8: Energy balances and annual performance for each climate (Strasbourg, Lyon and Nice) and each storage mode (water, RT58 and PEG6000)

4.3.2. PCM temperatures

The temperatures observed within the prototype are directly correlated with the identified melting ranges of the PCM. The melting range of PEG6000, which is narrower and higher in temperature than RT58, leads to much higher PCM temperature levels (figure 9 in Nice). This result shows the interest of the PEG6000 in limiting the use of back-up, thanks to a faster rise in temperature towards the DHW set point (sensible heat mobilized). The analysis carried out on the cavity leads to the same types of conclusions (see figure 5).

The comparison of storage temperatures must also consider the heat extracted from storage during withdrawals. Except for the PEG6000 in Nice, it is lower in the case of the two PCMs compared to water (figure 8), which could also explain the low level of water temperature in the storage compared to the two PCMs. Nevertheless, Figure 9 corresponds to similar quantities of energy extracted from the storage between the PEG6000 and water (case of Nice), and a clear difference is observed in the distribution of temperatures in the storage (lower for water).

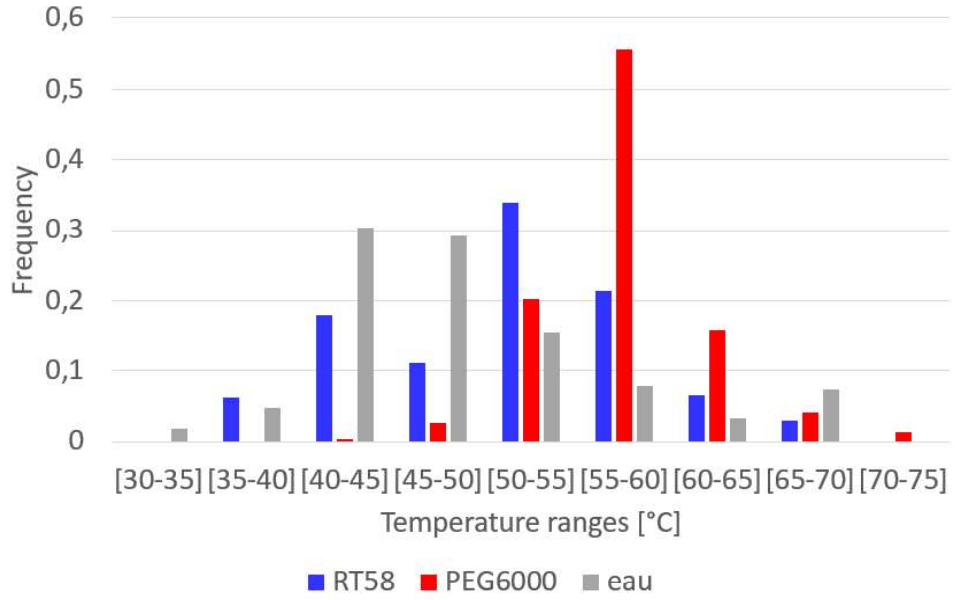

Figure 9: Average storage temperature (Nice)

4.3.3. Evolution of temperatures and powers during withdrawal

Figure 10 shows the variation of the heat flux transmitted from the RT58 to the water by the three DHW heat exchangers during a withdrawal of 6 minutes at 700l/h. Only the evolution of paraffin is presented knowing that the results with PEG6000 are similar. The maximum power value calculated with the water inlet-outlet temperatures is 23kW. This value is certainly underestimated in the first moments due to the inertia on the temperature measurement. The real profile rather corresponds to a rapid decrease in power for approximately 1 minute. This rapid decrease is followed by a much slower decrease linked to the evolution of the storage temperature. The power reaches 12.5kW at the end of the withdrawal. The outlet temperature of the exchanger goes through a maximum of 59°C (it should also follow a decrease from 60°C which is the initial temperature) to 37°C at the end of the withdrawal.

The first peak power can be explained by the rapid discharge phenomena (low inertia of the fins, of the heat exchangers and thin layer of PCM as is seen with the cavity in figure 5), knowing that the small volume of water contained in the heat exchangers empties in just a few seconds. The estimation of the exchange power during withdrawal without rapid effects is around 16kW for a flow rate of 700l/h when the RT58 is at 60°C (figure 11). Currently, even with a storage at 60°C, it is difficult to cover 100% of needs during “long” draw-offs for high flow rates. The discharge power is obviously conditioned by the effective thermal conductivity of the PCM integrating the fins. Reducing the fin pitch increases the effective conductivity, and therefore the power exchanged (figure 11).

Even if the power is currently not sufficient for the maximum flow rates considered when the duration of the withdrawal exceeds about 1 minute, we observe after the withdrawal the rise in temperature due to conduction. The recharging time is a few minutes (figure 10). This makes it possible to benefit fairly quickly during the next withdrawal, from the overpower obtained thanks to the initial discharge of the highly conductive components (fins, stainless steel exchanger) and a thin layer of PCM. Fractional water tapping is this beneficial for the solar fraction of the prototype in its current configuration.

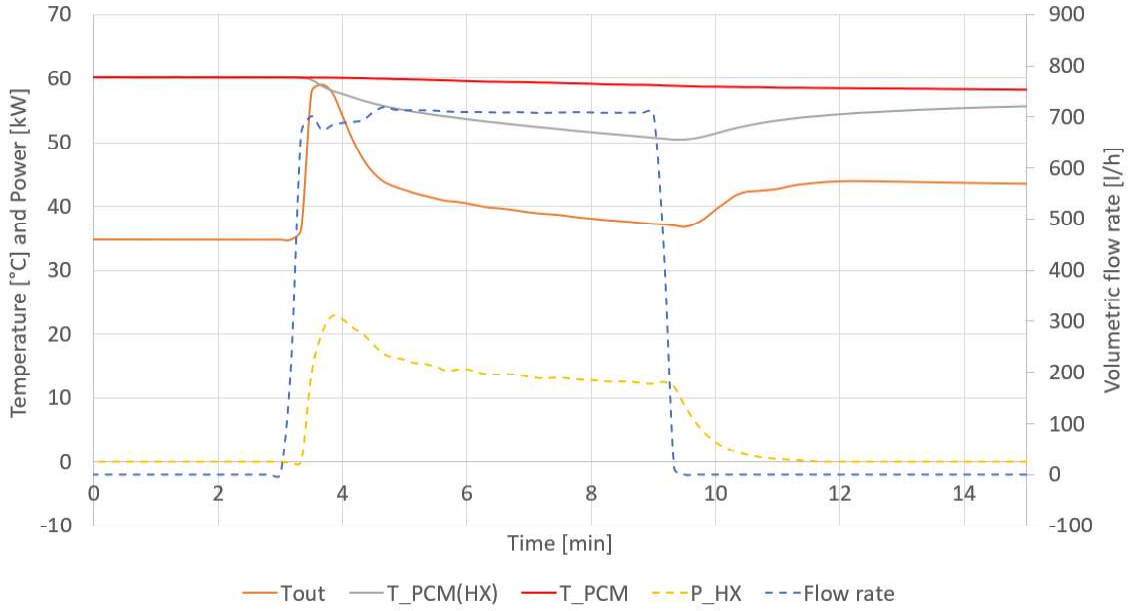

Figure 10: Example of withdrawal with initial temperature at 60°C (Lyon, RT58)

If we only consider the cooling of the fins and the heat exchangers at the very beginning of a withdrawal (rapid effect), the power supplied can be estimated with the thermo-physical characteristics of each element. The average value is around 4.5kW for a period of approximately 60 seconds.

In the case of the PEG6000, the latent heat dissipated during the recalescence phase (approximately 15% of the latent heat) represents an average power of 2kW for approximately 1500 seconds. To benefit from this, the PEG6000 must be entirely liquid, then it must be sufficiently cooled to a temperature that depends on the cooling rate (about 50°C). These conditions are obtained very occasionally in summer and it is likely that this power gain does not modify the annual solar fraction much. On the other hand, the fact of remaining liquid thanks to supercooling, as we saw in Nice, makes it possible to intensify exchanges and significantly improve annual solar coverage.

4.4. Improved prototype performance (target 25kW during discharge)

A parametric study of the exchanged power (without the fast effects) was carried out numerically as a function of the spacing δ [m] and the thickness t [m] of the fins for both the PEG6000 and the RT58 (figure 11). In the configuration of the prototype (δ=0.006m and t=0.0003m) and assuming a PCM temperature at 60°C, we obtain a power of 18kW for the PEG6000, and a slightly lower value for the RT58 (16kW) due to its lower thermal conductivity.

To reach 25kW (700l/h), the fin pitch must be 3.3mm instead of the current 6mm, which slightly increases the dimensions of the prototype. This doubles the weight of the fins (12 to 24 kg) knowing that the current weight of the prototype is 75 kg empty. Regarding the RT58, reaching 25kW is possible but for fin spacings less than 3mm due to its lower thermal conductivity. Figure 11 shows that it is more interesting to modify the spacing of the fins than the thickness of the fins to increase the withdrawal power. Increasing the heat flux with the thickness of the fins is not a good solution because it does not greatly improve the effective thermal conductivity of the PCM, which is the main factor limiting heat exchange.

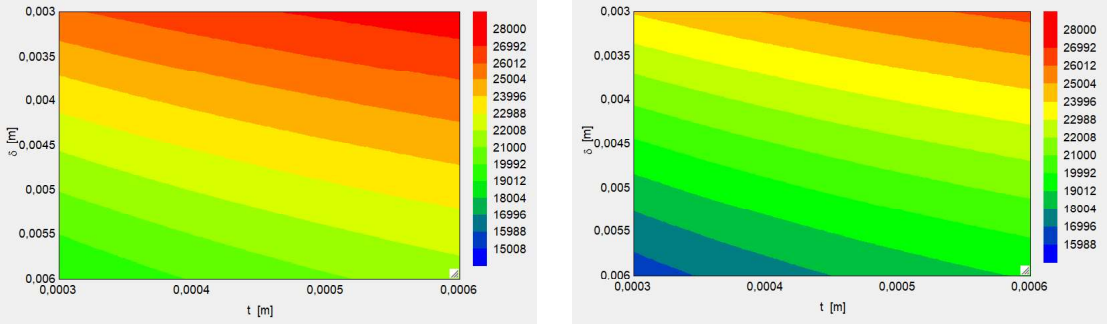

Figure 11: Effect of the spacing of the fins (δ) and their thickness (t) on the withdrawal power (Watt) considering storage at 60°C and a flow rate of 700l/h (PEG6000 on the left and RT58 on the right)

5. Conclusion and outlook

The fluxmeter bench made it possible to precisely identify the behavior laws (enthalpy as a function of temperature) of the two PCMs, both during melting and solidification. The accuracy of these laws is essential to correctly model a thermal storage. Here is what differentiates the two materials studied (RT58 and PEG6000):

- A higher thermal conductivity with PEG6000 ($\lambda_{PEG} = 1.7 * \lambda_{RT}$), which favors exchanged fluxes,
- A higher density with PEG6000 ($\rho_{PEG} = 1.36 * \rho_{RT}$), which promotes storage capacity,
- A narrower melting range with the PEG6000 (52-64°C compared to 30-62°C for the RT58), which makes it possible to reach the setpoint temperature more quickly (and therefore delay the use of back-up)
- A supercooling of about 12°C with PEG6000 (very low with RT58) which has a beneficial influence on the annual performance in Nice because the liquid state promotes heat exchange. On the other hand, we did not observe any impact of heat release during recalescence on the annual performance of the prototype.

Considering the values identified with the briquette (table 2 and figure 2), the PEG6000 stores more energy for a given volume than the RT58 (40% more over the 40-70°C range). Compared to water, the energy density gain with PEG6000 is 122% over the same temperature range.

As the mass*specific heat product of water is higher than PCM at equivalent volume, the PCM temperature increases faster during charging before the onset of melting. This point is very interesting because it limits the use of back-up in the case of PCM. This was clearly observed in the case of PEG6000. With the RT58, the onset of melting arriving quite early, the rise in temperature is generally slower than that of water.

The storage cavity with fins allows above all to increase the effective thermal conductivity of the PCM. It is much more efficient in terms of power extracted from the storage to use a large number of thin fins, rather than thicker and fewer fins. Logically, the rise in temperature observed is faster for PEG6000 than for RT58 due to the wide melting range of the latter, which begins at 30°C. The experiment with the cavity shows a stored energy 38% times greater for the PEG6000 between 20 and 70°C mainly due to the density ratio (1.36). This result is also consistent with the simplified representation of the stored volumetric energy (figure 2) which gives a difference of 34%. In terms of flux exchanged, it is globally higher for the PEG than the RT considering the differences in the conductivities and the quantities of energy stored. We observe for step charge a first similar peak for the two PCMs linked to the rapid effects of the fins and of a thin layer of PCM, and a second peak linked to the melting of the PCM. This second peak is more prominent in the case of PEG because the melting range of PEG is narrower. During discharge, a larger peak is observed for PEG during the recalescence phase.

The experimental results of the prototype obviously confirm the known limit of PCM concerning their low thermal conductivity, which can penalize the power extracted from the storage during prolonged withdrawals. It is therefore essential to consider the thermal conductivity of the PCM, which can be adjusted thanks to the spacing between the fins. The spacing of the fins plays a major role in heat transfer, compared to the thickness of the fins, which should rather be minimized for reasons of weight, and therefore cost. The evaluation of the annual performances carried out on the prototype (volume of 100 liters) shows that the solar fraction is quite satisfactory, between 43 and 87% depending on the climate. The comparison with a conventional solar DHW system (61 to 91% solar fraction for a storage volume of 150 liters of water) and the prototype shows poorer performance with the prototype

because the maximum flow of the conditions of the test is high with regard to the spacing of the fins. It would be enough to go from 6 to 3 mm in fin pitch to have the same level of performance as the classic system. Concerning the solar energy stored from collectors, the transmitted heat flows being less, the quantities of stored energy are equivalent between the prototype and the classic installation, with a 50% higher storage volume in the case of water (150 liters). The distribution of average temperatures observed within the PCM is directly correlated with the PCM melting ranges. The RT58 is thus penalized compared to the PEG6000 because the start of the fusion takes place at a much lower level (30°C against 52°C). For these two PCMs, the average temperature observed in the storage is higher than that of the water, which is very interesting with regard to the back-up system.

Outlook

Supercooling can be beneficial on one hand with the increase in power during discharge (liquid state and recalescence phase) and on the other hand, with the possibility of storing heat with very low thermal losses over long periods. On the other hand, supercooling can be penalizing if the latent heat is poorly valued according to the temperatures applied during charging and discharging. It is therefore important to clearly define the behavior laws representing all the phenomena. The behavior laws that have been considered [9] give more credibility to the results concerning the evaluation and optimization of PCM storage.

The current limits of the laws of thermodynamic behavior relate to the cycles of charges and partial discharges with supercooling. In this case, they must better model the kinetics of crystallization during multiple partial charge-discharge cycles and during simultaneous charge-discharge which ultimately correspond to the actual operating conditions. Going towards bio-based materials seems important to us in an ecological transition approach and it is likely that this kind of PCM will be confronted with complex behaviors.

The configuration tested experimentally with "high power back-up" works well with respect to solar fraction, knowing that it could be improved by adjusting the spacing of the fins. The initial choice was to propose a prototype corresponding to half of the necessary storage. The underlying idea was to double the storage for an actual solar installation. For financial reasons, we think at the end of this work that it is preferable to limit ourselves to the volume of the 100 liters of the prototype, and to adjust the discharge power by reducing the pitch of the fins to 3mm in order to benefit of sufficient DHW power. This solution could also be applied for a traditional electric tank (low power back-up), which we would like to transform into a solar DHW system. A volume of 100 liters of PCM could then easily be positioned in a closet or wasted space, and thus be less penalizing in terms of space.

Declaration of Competing Interest: The authors declare that they have no known competing financial interests or personal relationships that could have appeared to influence the work reported in this paper.

Funding: This research was funded by the French Association National de la Recherche (ANR) for the EUROPA project, grant number ANR-18-CE05-0034-01.

Acknowledgments: This study is a part in the EUROPA research project funded by the ANR (French National Research Agency).

References

[1] N. Nallusamy, S. Sampath, and R. Velraj. Experimental investigation on a combined sensible and latent heat storage system integrated with constant/varying (solar) heat sources. Renewable Energy, 32(7) :1206–1227, June 2007.

[2] M.Y. Abdelsalam, H.M. Teamah, M.F. Lightstone, and J.S. Cotton. Hybrid thermal energy storage with phase change materials for solar domestic hot water applications : Direct versus indirect heat exchange systems. Renewable Energy, 147 :77–88, March 2020.

[3] I. Al-Hinti, A. Al-Ghandoor, A. Maaly, I. Abu Naqeera, Z. Al-Khateeb, and O. Al-Sheikh. Experimental investigation on the use of water-phase change material storage in conventional solar water heating systems. Energy Conversion and Management, 51(8) :1735–1740, August 2010.

[4] Abdul Jabbar N. Khalifa, Kadhim H. Suffer, and Mahmoud Sh. Mahmoud. A storage domestic solar hot water system with a back layer of phase change material. Experimental Thermal and Fluid Science, 44 :174–181, January 2013.

[5] Mouna Hamed, Ali Fallah, and Ammar Ben Brahim. Numerical analysis of charging and discharging performance of an integrated collector storage solar water heater. International Journal of Hydrogen Energy, 42(13) :8777–8789, March 2017.
[6] Matteo Bilardo, Gilles Fraisse, Mickael Pailha, Enrico Fabrizio. Modelling and performance analysis of a new concept of integral collector storage (ICS) with phase change material. Solar Energy, Volume 183, 1 May 2019, Pages 425-440
[7] Robynne E. Murray and Dominic Groulx. Experimental study of the phase change and energy characteristics inside a cylindrical latent heat energy storage system : Part 2 simultaneous charging and discharging. Renewable Energy, 63 :724–734, March 2014.
[8] Radouane Elbahjaoui and Hamid El Qarnia. Thermal performance of a solar latent heat storage unit using rectangular slabs of phase change material for domestic water heating purposes. Energy and Buildings, 182 :111–130, January 2019
[9] Thonon M., Fraisse G. , Zalewski L. , Pailha M. , Towards a better analytical modelling of the thermodynamic behaviour of phase change materials, Journal of Energy Storage. 32 (2020) 101826. https://doi.org/10.1016/j.est.2020.101826
[10] Younsi, Z.; Zalewski, L.; Lassue, S.; Rousse, D.R.; Joulin, A. A Novel Technique for Experimental Thermophysical Characterization of Phase-Change Materials. Int J Thermophys 2011, 32, 674–692, doi:10.1007/s10765-010-0900-z.
[11] Franquet, E.; Gibout, S.; Tittelein, P.; Zalewski, L.; Dumas, J.-P. Experimental and Theoretical Analysis of a Cement Mortar Containing Microencapsulated PCM. Applied Thermal Engineering 2014, 73, 32–40, doi:10.1016/j.applthermaleng.2014.06.053. https://doi.org/10.1016/j.tsep.2022.101336.
[12], L.; Franquet, E.; Gibout, S.; Tittelein, P.; Defer, D. Efficient Characterization of Macroscopic Composite Cement Mortars with Various Contents of Phase Change Material. Applied Sciences 2019, 9, 1104, doi:10.3390/app9061104.
[13] Maxime Thonon, Gilles Fraisse, Laurent Zalewski, Mickael Pailha. Analytical modelling of PCM supercooling including recalescence for complete and partial heating/cooling cycles. Applied Thermal Engineering 190 (2021) 116751
[14] Hasan Sayegh, Antoine Leconte, Gilles Fraisse, Etienne Wurtz, Simon Rouchier. Computational time reduction using detailed building models with Typical Short Sequences. Energy, 2022, Volume 244, 14 pages
[15] Jesus Lizana, Pedro E. Sanchez-Jimenez, Ricardo Chacartegui, Jose A. Becerra, Luis A. Perez-Maqueda. Supercooled sodium acetate aqueous solution for long-term heat storage to support heating decarbonisation. Journal of Energy Storage, Volume 55, Part B, 15 November 2022, 105584
[16] Xiaoxiang Li, Jingyi Zhang, Yizhe Liu, Yangzhe Xu, Kehang Cui, Zhenpeng Yao, Benwei Fu, Chengyi Song, Wen Shang, Peng Tao, Tao Deng. Supercooled sugar alcohols stabilized by alkali hydroxides for long-term room-temperature phase change solar-thermal energy storage. Chemical Engineering Journal, Volume 452, Part 3, 15 January 2023, 139328
[17] Moeini Sedeh, M.; Khodadadi, J.M. Thermal Conductivity Improvement of Phase Change Materials/Graphite Foam Composites. Carbon 2013, 60, 117–128, doi:10.1016/j.carbon.2013.04.004.
[18] Li, M.; Guo, Q.; Su, Y. The Thermal Conductivity Improvements of Phase Change Materials Using Modified Carbon Nanotubes. Diamond and Related Materials 2022, 125, 109023, doi:10.1016/j.diamond.2022.109023.
[19] Xu, C.; Zhang, H.; Fang, G. Review on Thermal Conductivity Improvement of Phase Change Materials with Enhanced Additives for Thermal Energy Storage. Journal of Energy Storage 2022, 51, 104568, doi:10.1016/j.est.2022.104568.
[20] Mariam Jadal, Jérôme Soto, Didier Delaunay. Thermal conductivity evolution of a compressed expanded natural graphite – Phase change material composite after thermal cycling, Thermal Science and Engineering Progress, Volume 28, 1 February 2022
[21] Maxime Thonon. Étude d'un échangeur-stockeur avec matériaux à changement de phase pour le stockage d'eau chaude sanitaire. Thèse de doctorat de l'Université Savoie Mont-Blanc, soutenue le 30/11/2021, 218 pages.
[22] Thonon Maxime, Laurent Zalewski, Stephane Gibout, Erwin Franquet, Gilles Fraisse, Mickael Pailha. Experimental comparison of three characterization methods for two phase change materials suitable for domestic hot water storage. Applied Sciences. 2021, 11(21), 10229; https://doi.org/10.3390/app112110229
[23] Yefim Ivshin and Thomas J. Pence. A constitutive model for hysteretic phase transition behavior. Int. J. Engn Sci., 32(4) :681–704, 1994.
[24] Tilman Barz, Johannn Emhofer, Klemens Marx, Gabriel Zsembinszki, and Luisa F. Cabeza. Phenomenological modelling of phase transitions with hysteresis in solid/liquid PCM. Journal of Building Performance Simulation, 12(6) :770–788, November 2019.

[25] Mariam Jadal, Jérôme Soto, Nicolas Boyard, Didier Delaunay, Experimental determination of crystallization kinetic model of CENG-PCM composite material. Validation at macro and meso scales, Thermal Science and Engineering Progress, Volume 33, 2022, 101336, ISSN 2451-9049,

Declaration of Interest Statement

Date : 30th of June (2023)

Author names: Gilles Fraisse, Maxime Thonon, Mickael Pailha, David Cloet, Laurent Zalewski, Antoine Leconte, Eric François, Robert Moracchioli, Luc Traonvouez

Manuscript title: PERFORMANCE COMPARISON OF TWO PCM CANDIDATES FOR NEW CONCEPT OF COMPACT THERMAL STORAGE IN SDHW SYSTEMS

The authors declare that they have no known competing financial interests or personal relationships that could have appeared to influence the work reported in this article